www.czasopisma.pan.pl PAN POLSKA AKADEMIA NAUK www.journals.pan.pl

ARCHIVES OF ACOUSTICS
36, 3, 533–544 (2011)

DOI: 10.2478/v10168-011-0038-4

Effect of Transverse Acoustic Flow on the Input Impedance of Rapidly Flaring Horns[1]

Cornelis J. (Kees) NEDERVEEN

Acacialaan 20
2641 AC Pijnacker, The Netherlands
e-mail: cjnederv@xs4all.nl

(*received January 11, 2011; accepted May 30, 2011*)

In slowly flaring horns the wave fronts can be considered approximately plane and the input impedance can be calculated with the transmission line method (short cones in series). In a rapidly flaring horn the kinetic energy of transverse flow adds to the local inertance, resulting in an effective increase in length when it is located in a pressure node. For low frequencies corrections are available. These fail at higher frequencies when cross-dimensions become comparable to the wavelength, causing resonances in the cross-direction. To investigate this, the pipe radiating in outer space is modelled with a finite difference method. The outer boundaries must be fully absorbing as the walls of an anechoic chamber. To achieve this, Berenger's perfectly matched layer technique is applied. Results are presented for conical horns, they are compared with earlier published investigations on flanges. The input impedance changes when the largest cross-dimension (outer diameter of flange or diameter of the horn end) becomes comparable to half a wavelength. This effect shifts the position of higher modes in the pipe, influencing the conditions for mode locking, important for ease of playing, dynamic range and sound quality.

Keywords: input impedance, horn, wind musical instruments, boundary conditions.

1. Introduction

Most wind instruments are nearly cylindrical or conical. Sometimes they are provided of a horn at the open end, supposedly for increasing the radiation to the surroundings, though the trumpet, definitely louder than a flute, would not need this (see Fig. 1).

Since a horn is a bore perturbation over a certain length, its influence is dependent on the mode so it may have a function in the tuning of the instrument. A cylindrical flute has a long gradual taper toward the embouchure, which

[1] This paper was presented at the Vienna Talk 2010 conference (Nederveen, 2010)

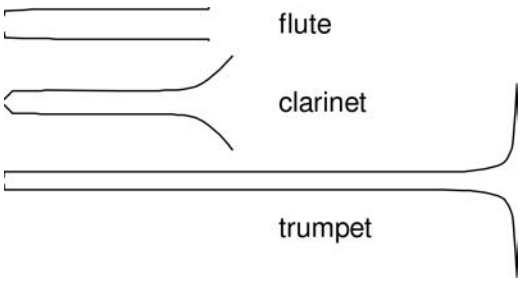

Fig. 1. Three wind instruments with and without horns at the radiating open end (x and y scales are different).

influences the tuning between the modes; a clarinet ends in a catenoidal horn which compensates for the tuning shifts in the second register due to the speaker hole and the volume of the closed holes (Nederveen, 1998). In both cases the bore changes are sufficiently gradual to allow assuming wave fronts to be approximately plane and using the transmission line (TL) method (short cones in series) for calculating the input impedance. Figure 2 shows a basic situation of a cylinder of length L_a joined to a cone of length L_{ba}. The input radius of the cone is a, its output radius b. For low frequencies, assuming the horn short with respect to the wavelength, applying the TL method, the cone can be described as a length correction L_e to the cylinder of

$$L_e = (a/b)\left[L_{ba} + (a/b)L_b\right], \tag{1}$$

where in the case of an unflanged open end, $L_b = 0.613b$ (Nederveen, Dalmont, 2008).

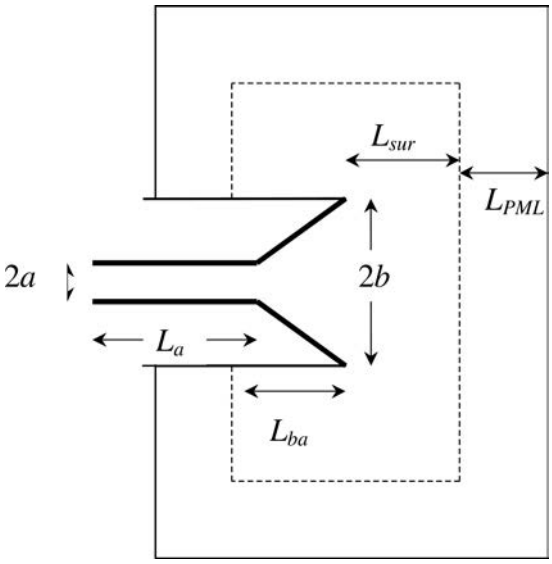

Fig. 2. Dimensions of a cylinder with a short cone.

When the flare of the horn is large there will be cross flow which demands kinetic energy. In that case we may apply a fit formula for an extra series impedance to be added to the input impedance of the conical tube piece (Nederveen, Dalmont, 2008).

$$Z_{\text{extra}} = \frac{j\rho c}{\pi a^2}\,\frac{a}{b}\,kL_{ba}\left[\sqrt[1.6]{1+\left(\frac{0.821(b-a)}{L_{ba}}\right)^{1.6}}-1\right]. \tag{2}$$

The correction becomes important for $(b-a)/L_{ba} > 0.1$. This expression can be used successfully up to $L_{ba} = 0$ (flanges). It fails at higher frequencies where resonances occur in the transverse direction. Investigating this was the aim of the present study.

An indication of what may happen can be seen from a previous study of the end correction of a flange. It was found that resonances across the flange change the end correction irregularly (Dalmont *et al.*, 2001). Results are given in Fig. 3 for a circular flange with $b = 5a$. As can be observed, a peak in L_e/a occurs at $ka \approx 0.3$, or $kb \approx 1.5 \approx \pi/2$, approximately a quarter-wavelength.

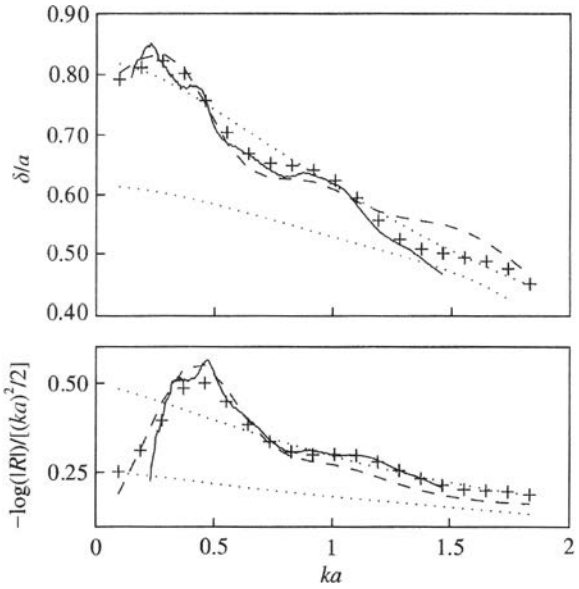

Fig. 3. End correction δ (or L_e) for a flange, divided by the pipe radius a, as a function of ka; Flange radius $b = 5a$. Top: real part; bottom: imaginary part/(ka). Dotted lines: theory for infinite and zero flange; ++: calculation with boundary element method; drawn line: measurements, dashed line: fit formula (Nederveen, Dalmont, 2008).

This also can be expected to happen in a short horn at the end of a trumpet, which resembles a flange. This may influence the positions of the higher overtones. The exact positions of these overtones is important, they should preferably

be close to harmonically related because of the coupling to the excitation, which has a harmonic spectrum.

The present paper describes studies on conical horns attached to a cylindrical tube. They were made in the workshop of the Laboratoire d'Acoustique de l'Université du Maine in Le Mans, France. Their input impedance spectra were measured in the anechoic chamber of the Le Mans laboratory. Input impedances were calculated with the TL method without (called 1D) and with (called 3D) cross-flow correction, and with the finite difference method (FDM). The results obtained by the various methods are compared.

2. The Finite Difference Method (FDM)

The Helmholtz equation describes the sound field in the pipe and the open space it radiates into. In the finite difference method (FDM) grid points are fitted in the domain for which in three-dimensional Cartesion space discretization equations are set up for every point:

$$\sum_{1}^{6} \frac{p_n - p_0}{h_n^2} + k^2 p_0 = 0. \tag{3}$$

When the grid is uniform, $h_n = h$. Since the pipes are rotationally symmetric, cylindrical co-ordinates are used to make the field two-dimensional, saving on computer capacity (Nederveen, Dalmont, 2008). Taking the axial (z) direction 2–4 and the radial (r) direction 1–3, the discretization equation is (see Fig. 4)

$$\sum_{1}^{4} \frac{p_n - p_0}{h_n^2} + \frac{p_3 - p_1}{r(h_3 + h_1)} + k^2 p_0 = 0. \tag{4}$$

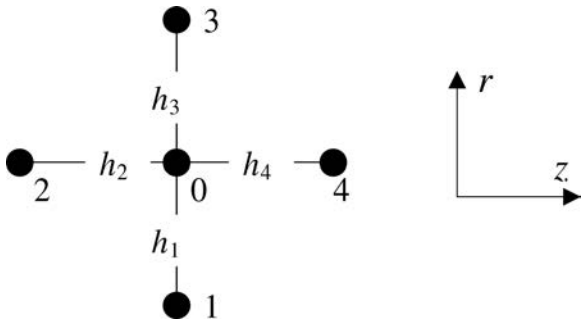

Fig. 4. Computational module for FDM calculations.

In the horn, the points are fitted to the curved walls of the pipe in a stepwise manner. To save on computer capacity the outer space must be bounded in some way. For a smooth transfer in the first outer layer of thickness L_{sur} (for

example 10 points) the same equation is used. In the next layer of thickness L_{PML} Berenger's PML (perfectly matched layer) technique is used. In this layer, absorption gradually increases, mimicking the absorbing walls of an anechoic chamber. There are various ways to implement this (Berenger, 1994; Yan *et al.*, 1997; Taflove, Hagness, 2005). It appeared most convenient to make the grid spacing progressively complex to the outside. For example, if the PML absorbing layer is extending to the right the grid dimensions become

$$h_4 = h\left(1 - 5i(m/m_{\max})^3\right). \tag{5}$$

where m is the layer number and $m_{\max}$ the thickness of the absorbing layer (for example 10 units).

The limited accuracy due to the discretization is improved by plotting the results against the reciprocal of the number of points and extrapolating to zero, yielding an estimate for an infinite number of points.

3. Results

As an introductory example we show some results of a FDM calculation for a combination of a conical pipe attached to a short cylinder with dimensions (symbols explained in Fig. 2)

$$[L_a \quad a \quad L_{ba} \quad b \quad L_{\mathrm{sur}} \quad L_{\mathrm{PML}}] = [1 \quad 3 \quad 22 \quad 12 \quad 15 \quad 30]. \tag{6}$$

In Figs. 5 and 6 the field lines of the pressure are plotted in 2D and 3D for $ka = 1.2$ (approximately 6600 Hz). Because of the requirements of the computing and plotting programs, cell numbering and pipe dimensions do not coincide and

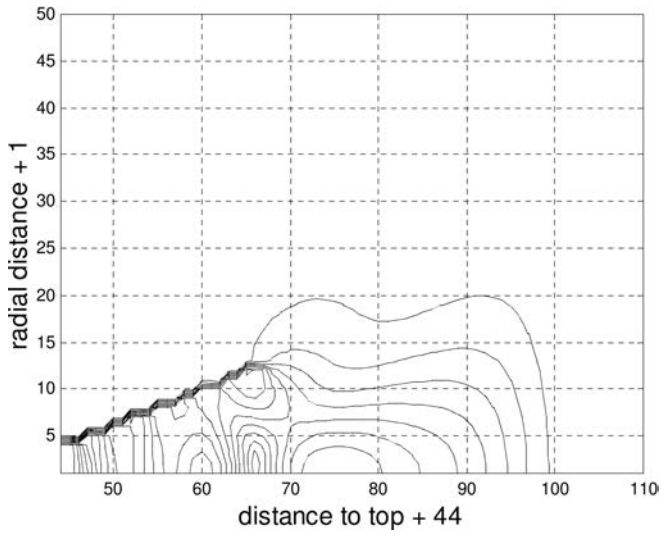

Fig. 5. Two-dimensional plot of the lines of equal pressure in a cylinder-cone combination.

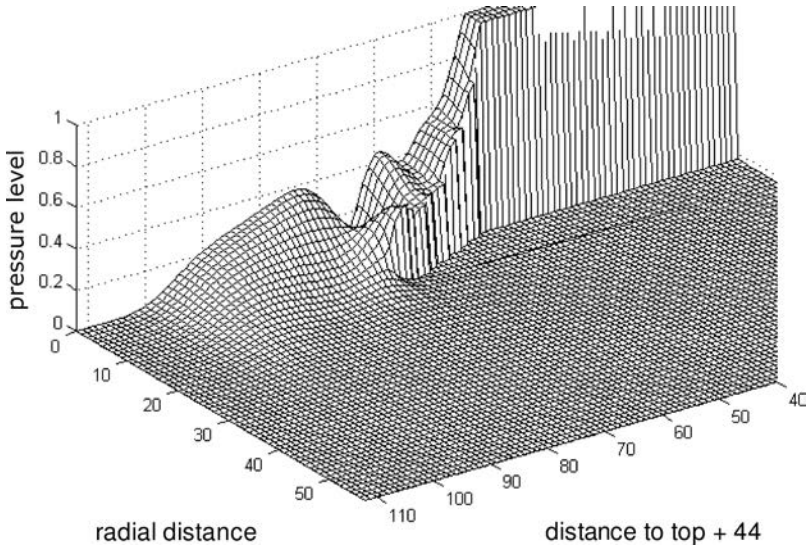

Fig. 6. Three-dimensional plot of pressure field in a cylinder-cone combination. The cone is to the left of the cylinder.

the pressure level backwards of the pipe entrance has been set to unity. Apart from these cosmetic shortcomings, the presence of waves in the transverse direction is apparent. It also can be observed that the pressure smoothly goes to zero toward the boundaries, no unwanted waves due to reflections are visible.

3.1. Cylinder with a long conical horn

The dimensions of the first cylinder/cone combination investigated (sketched in Fig. 7), are in mm

$$[L_a \quad a \quad L_{ba} \quad b] = [88 \quad 9.9 \quad 75 \quad 39.5]. \tag{7}$$

Although the same dimensions could be chosen for the FDM tube, this would seriously complicate the grid. Instead, a choice of slightly different dimensions leads to whole numbers:

$$[L_a \quad a \quad L_{ba} \quad b \quad L_{\text{sur}} \quad L_{\text{PML}}] = M[18 \quad 2 \quad 15 \quad 8 \quad 10 \quad 20]. \tag{8}$$

M is a multiplier increasing the number of points and consequently the accuracy; it is bounded by the computer capacity, is this case $M \leq 8$. Results in Fig. 8 pertain to $M = 4$.

Measurements on the various pipe combinations were performed at a temperature of 21°C. So in all calculations the velocity of sound at that temperature was assumed, viz. 343 m/s. FDM calculations were performed for $ka = 0.02{:}0.01{:}1.4$, corresponding to a frequency range between 110 and 7700 Hz. Impedances obtained in the four ways described above are plotted in Fig. 8. The relative positions of the peaks are given in Fig. 7. The ratios of the peak positions for the 1D

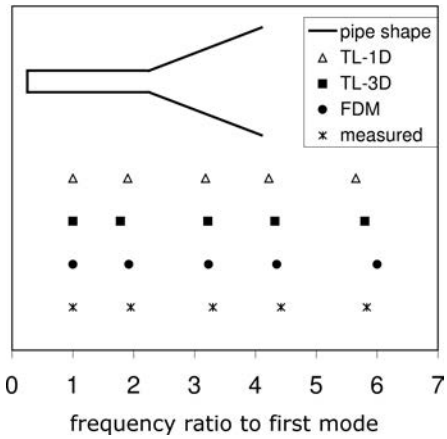

Fig. 7. Absolue value of input impedance as a function of frequency for a cylinder with a long cone, determined in four different ways (vertically shifted).

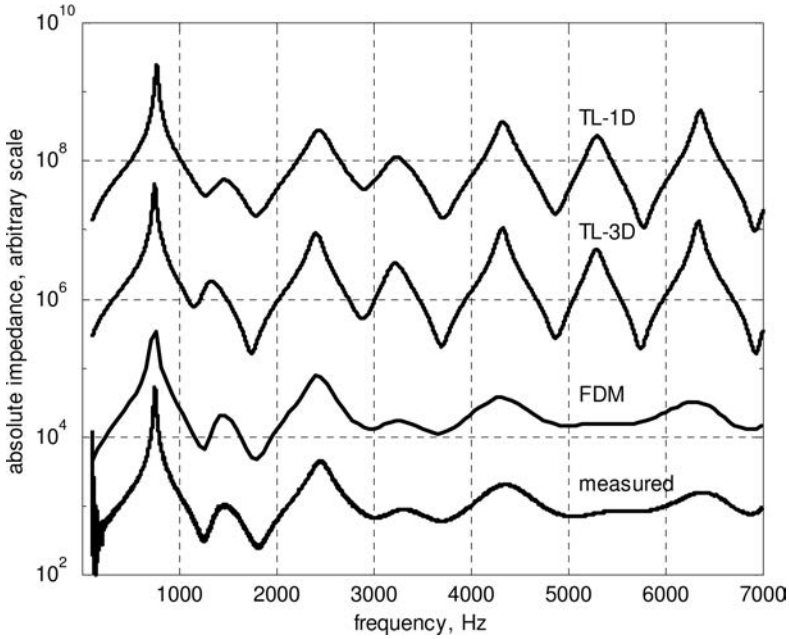

Fig. 8. Shape of the combination of cylinder with long cone, Relative positions of modes in a cylinder with a long cone.

and 3D TL methods changes; because the horns are rather long and the inertance corrections have an effect dependent of the position in the sound field.

It can be observed that the peaks of both the FDM and the measurements flatten out above 4500 Hz. This approximately corresponds to a wavelength of the exit diameter of the horn, 80 mm. Apparently, resonances in the cross direction destroy the resonances predicted by the TL methods.

The cone can be considered as a length correction to the cylinder, the correction coefficient is is plotted in Fig. 9. Its value at zero (extrapolated) = 2.15. The value earlier published by Nederveen and Dalmont (2008) is 2.33. Calculated with the approximate Eq. (1) gives $L_e/a = 2.03$.

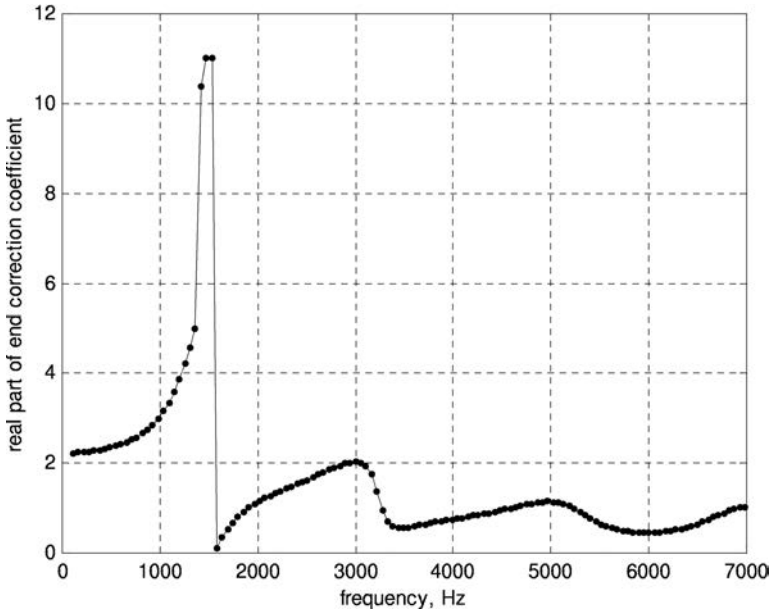

Fig. 9. Real part of the end correction coefficient L_e/a to the cylinder for the long cone, obtained by FDM.

Table 1 gives the positions of the first peak of the resonance spectrum obtained with the various methods. The value of the 1D-TL calculation is higher, due to neglect of the transverse flow energy in the horn. TL-3D and FDM correspond better and are closer to the measured value. There may be a systematic difference, which needs to be studied. It can be due to uncertainties in dimensions and/or temperature (see the Discussion).

Table 1. Position of first resonance peak for a cylinder with a long cone obtained with various methods.

Method	Measured	TL-1D	TL-3D	FDM
1st peak, Hz	748	766	746	744
Difference		+2.4%	−0.3%	−0.5%

3.2. Cylinder with a short conical horn

A second cylinder investigated was one with a short conical horn as sketched in Fig. 10. The dimensions in mm are:

$$[L_a \quad a \quad L_{ba} \quad b] = [89.8 \quad 10 \quad 12 \quad 19.9]. \tag{9}$$

For the FDM model we chose (in units)

$$[L_a \quad a \quad L_{ba} \quad b \quad L_{\text{sur}} \quad L_{\text{PML}}] = M[45 \quad 5 \quad 6 \quad 10 \quad 20 \quad 40], \tag{10}$$

where $M = 2$. Results are given in Figs. 10 and 11 and in Table 2. Impedance calculations and measurements are plotted in Fig. 11. Figure 10 gives relative positions of the peaks. Modes are approximately odd harmonics. At 6 kHz the

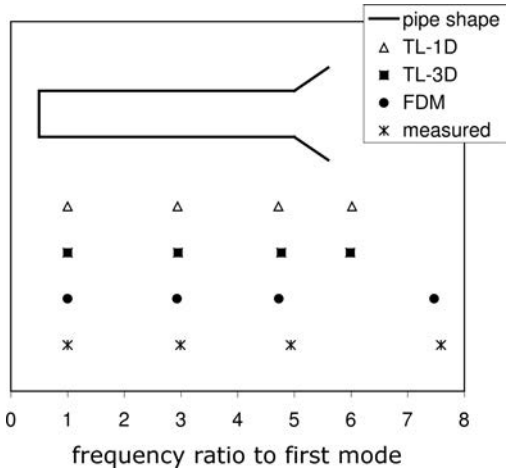

Fig. 10. Absolute value of imput impedance of a cylinder with a short cone.

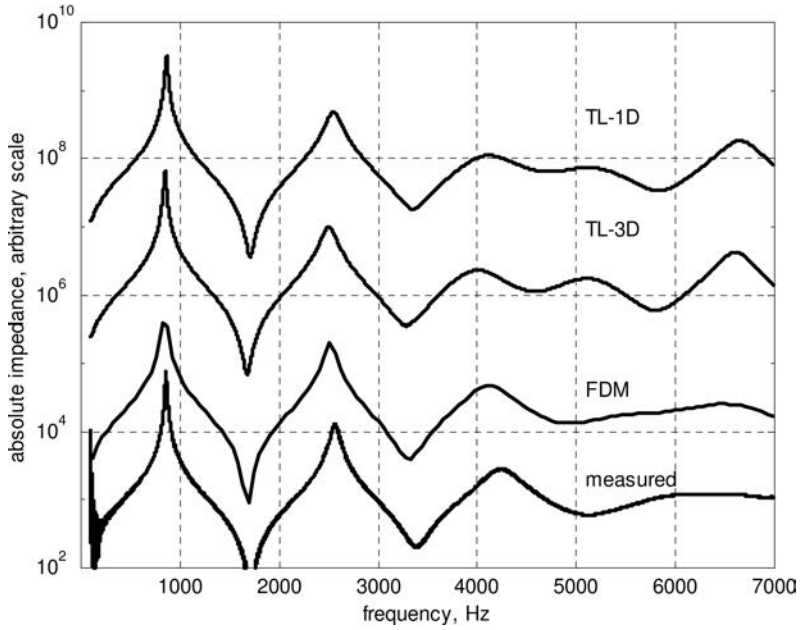

Fig. 11. Shape of the combination of cylinder and short cone. Relative positions of modes in a cylinder with a short cone.

peaks of both FDM and measurements flatten out, as compared with the TL calculations. Table 2 gives the positions of the first impedance peaks. As with the previous horn combination, the first peak shifts when the 3D correction is added to the TL method. As appears from Fig. 10, all peaks shift more or less the same; the horn is short, its effects is an extra inertance which is not very dependent on the frequency, contrary what is observed in Fig. 7 for the previous combination

Table 2. First resonance peak for a cylinder with a short conical horn.

Method	Measured	TL-1D	TL-3D	FDM
1st peak, Hz	859	865	850	855
Difference		+0.7%	−1%	−0.5%

The end correction coefficient to the cylinder can be calculated (Fig. 12). Its value is nearly constant below 5 kHz, at zero frequency $L_e/a \approx 1.1$. Above that frequency it abruptly decreases. Equation (1) gives 0.9.

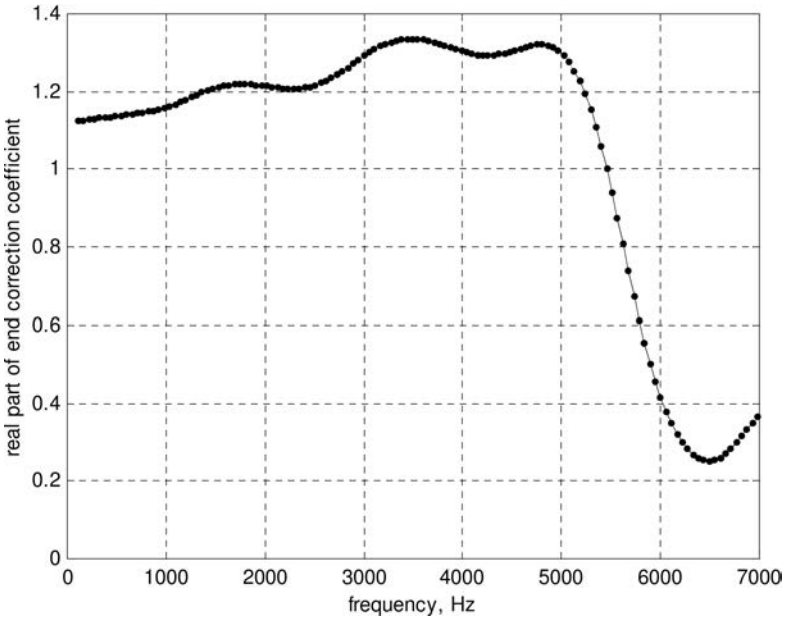

Fig. 12. Real part of the end correction coefficient L_e/a to the cylinder for the short cone, obtained by FDM.

4. Discussion

To get an impression of the absolute accuracy of the methods, a cylinder without horn is investigated. Both TL methods gives a value for the first peak

about 0.5% lower than the measured value. The FDM gave a value 0.3% higher. The deviations may be due to dimensional and temperature uncertainties. This needs to be investigated in detail. At this stage of the investigations the accuracy is estimated to be ± 0.5%.

The transition line (TL) method is very useful for the calculation of the first resonance peak of the impedance spectrum. In the case of a rapidly flaring horn a 3D correction is effective: the value found with TL-1D can be too high. A short conical horn can be described as a length correction, in a way comparable to that of a flange, provided the frequency is not too high. For a longer horn, resonances can occur in length as a well as in cross direction and complicate the simple picture. At higher frequencies the FDM results correspond much better with the measurements than the TL methods. TL methods are fast and conveniently applied. The FDM is cumbersome, a program must be written, there are limitations to the choice of the dimensions.

5. Conclusions

For calculating the input impedance of an arbitrary pipe, we conclude that

1. The well-known TL-1D method is useful for pipes flaring not too much.
2. For horns flaring more than 10% a correction for transverse flow, leading to the so-called TL-3D method is useful for low frequencies.
3. For higher frequencies, where cross-dimensions are no longer small with respect to the wavelength, the FDM gives better results. This method, however, is cumbersome.
4. Berenger's PML absorbing boundary can be implemented successfully in a FDM calculation scheme.

Acknowledgments

I thank Alex de Bruijn and Jean-Pierre Dalmont for many stimulating discussions, the latter also for valuable assistence with measuring the impedances.

References

1. Berenger J.P. (1994), *A perfectly matched layer for the absorption of electromagnetic waves*, J. Computational Physics, **114**, 1, 185–200.
2. Dalmont J.-P., Nederveen C.J., Joly N. (2001), *Radiation impedance of tubes with different flanges: numerical and experimental investigations*, J. Sound and Vibration, **244**, 3, 505–534.
3. Nederveen C.J. (1998), *Acoustical Aspects of woodwind instruments*, 2nd edition, Northern Illinois University Press, De Kalb, Ill, 78–79.

4. Nederveen C.J., Dalmont J.-P. (2008), *Corrections to the Plane-Wave Approximation in Rapidly Flaring Horns*, Acta Acustica/Acustica, **94**, 3, 461–473.

5. Taflove A., Hagness S.C. (2005), *Computational Electrodynamics*, Artech House, Norwood, 273–328.

6. Yuan X., Borup D., Wiskin J.W., Berggren M., Eidend R., Johnson S.A. (1997), *Formulation and validation of Berenger's PML absorbing boundary for the FDTD simulation of acoustic scattering*, IEEE Transactions on Ultrasonics, Ferroelectrics, and Frequency Control, **44**, 4, 816–822.